PHILOSOPHICAL TRANSACTIONS OF THE ROYAL SOCIETY A

Phil. Trans. R. Soc. A (2008) **366**, 4253–4271
doi:10.1098/rsta.2008.0194
Published online 30 September 2008

Experiments on metal–silicate plumes and core formation

By Peter Olson[1,*] and Dayanthie Weeraratne[2,†]

[1]*Department of Earth and Planetary Sciences, Johns Hopkins University, Baltimore, MD 21218, USA*
[2]*Department of Terrestrial Magnetism, Carnegie Institution, Washington, DC 20015, USA*

Short-lived isotope systematics, mantle siderophile abundances and the power requirements of the geodynamo favour an early and high-temperature core-formation process, in which metals concentrate and partially equilibrate with silicates in a deep magma ocean before descending to the core. We report results of laboratory experiments on liquid metal dynamics in a two-layer stratified viscous fluid, using sucrose solutions to represent the magma ocean and the crystalline, more primitive mantle and liquid gallium to represent the core-forming metals. Single gallium drop experiments and experiments on Rayleigh–Taylor instabilities with gallium layers and gallium mixtures produce metal diapirs that entrain the less viscous upper layer fluid and produce trailing plume conduits in the high-viscosity lower layer. Calculations indicate that viscous dissipation in metal–silicate plumes in the early Earth would result in a large initial core superheat. Our experiments suggest that metal–silicate mantle plumes facilitate high-pressure metal–silicate interaction and may later evolve into buoyant thermal plumes, connecting core formation to ancient hotspot activity on the Earth and possibly on other terrestrial planets.

Keywords: Earth's core; core formation; magma ocean; metal–silicate plumes

1. Introduction

Evidence from short-lived isotopes indicates that the Earth accreted from smaller planetesimal objects in a relatively short period of time, estimated at 30–40 Myr (Wood *et al.* 2006). Meteorite evidence also indicates that some of these accreting objects were massive and already had differentiated metallic cores of their own, which were formed within a few Myr time (Klein *et al.* 2002). The large gravitational energy flux accompanying such rapid accretion implies that a transient magma ocean could have been maintained to a considerable depth in the Earth (Solomatov 2000). The impact of large objects would inject enormous

* Author for correspondence (olson@jhu.edu).
† Present address: Department of Geological Sciences, California State University, Northridge, CA 91330, USA.

One contribution of 14 to a Discussion Meeting Issue 'Origin and differentiation of the Earth: past to present'.

amounts of kinetic and potential energy into the magma ocean, creating a highly turbulent fluid environment in which the segregation of the core material from the mantle material takes place (Rubie *et al.* 2003, 2007).

If the core of a differentiated planetesimal remained coherent following impact with the Earth, it would quickly sink through the magma ocean, and assuming that the magma ocean did not extend to the core, the metal would then descend through the underlying crystalline mantle by one of several possible mechanisms, including fracture propagation (Stevenson 1990) or as large diapirs derived from Rayleigh–Taylor instabilities (Elsasser 1963; Ida *et al.* 1987). Although such direct transport of large metal volumes into the core probably did occur, the evidence in favour of metal–silicate chemical re-equilibration suggests that this was not the norm. Instead, the mantle abundance of siderophile elements such as Ni and Co suggests that there was a post-impact phase characterized by some amount of chemical equilibrium between metal and silicates (Chabot *et al.* 2005). Element partitioning indicates this re-equilibration occurred at elevated temperature (approx. 2500 K) and relatively high pressures, in the region of 30–40 GPa (Righter & Drake 2000).

Equilibration between metals and upper mantle silicates at high pressure prior to the final stage of core segregation places some important constraints on the core formation process. It requires that large planetesimal objects disaggregate at the time of or shortly after their impact. The rate of extraction of siderophile elements from liquid metals is limited by their mass diffusivity, which is typically $10^{-9}\,\mathrm{m}^2\,\mathrm{s}^{-1}$ or less. Even if the siderophile extraction process is accelerated by the presence of thin interfacial layers, their low mass diffusivity limits the size of liquid metal drops or filaments that could equilibrate with the magma to a fraction of a metre or smaller (Rubie *et al.* 2003). Such small metal volumes cannot descend a substantial distance through crystalline mantle unless there is a permeable network already in place. Although it is possible that such a network might develop in the solid mantle (Yoshino *et al.* 2003) it requires a combination of small dihedral angles between the molten metal and the solid silicates for permeability, a substantial melt fraction or porosity, and also large shear stresses in the solid (Honda *et al.* 1993). This particular combination is most likely to occur near the base of the crystalline mantle rather than near its top, because the dihedral angle at lower pressures may be too large to produce the necessary permeability (Rubie *et al.* 2007).

Other important constraints on the segregation mechanism are the superheated state of the core today and the power requirements of the geodynamo in the past. Core superheat is the excess potential temperature of the core compared with its melting temperature at surface pressure. Based on the present-day geotherm, the core superheat is now approximately 1000 K. According to thermal evolution models of the core, however, it may have been twice this large at the time of the core segregation. In order to power the geodynamo, the core must lose substantial heat to the mantle, in the range of 4–10 TW (Nimmo 2007). This implies that the average temperature of the core was far higher in the early Earth, particularly when the solid inner core had not yet nucleated and the geodynamo probably relied on thermal convection alone (Labrosse *et al.* 2001). We note that a large initial core superheat is not easily reconciled with percolation as the primary core formation mechanism, because the core material would have come into approximate thermal equilibrium with the colder primitive mantle.

In this paper, we examine some fluid dynamical processes of core segregation using laboratory experiments. We use concentrated and dilute sucrose solutions (corn syrups) to represent the crystalline mantle and the magma ocean, respectively, and liquid gallium to represent the core-forming metals. Gravitational segregation in this environment occurs through the formation of negatively buoyant, mixed-composition structures that we call metal–silicate plumes. These plumes form naturally in the three-fluid system of our experiments, and we demonstrate that metal–silicate plumes in the early Earth can provide a means for metals dispersed in the near-surface magma ocean to descend rapidly to the core, even through a very viscous primitive mantle. We show that metal–silicate plumes are highly dissipative structures, and can result in large core superheat while simultaneously allowing for some degree of high-pressure core–mantle chemical re-equilibration. Finally, we argue that descending metal–silicate plumes tend to evolve into ascending silicate plumes with time, suggesting that the earliest dynamics of the deep mantle may have been plume dominated.

2. Experimental methods

We consider the dynamics of liquid gallium in a more viscous but less dense layered fluid (corn syrup–water solutions) in three different situations that are relevant to the core segregation process. First, we examine the motion of a single drop of liquid gallium as it crosses the stable interface between a low-density, less viscous diluted syrup solution (representing the magma ocean) and a high-density, more viscous concentrated syrup solution (representing the crystalline mantle). Second, we examine the instability of a gallium layer at the interface between dilute and concentrated syrup solutions. Finally, we consider the instability of a gallium emulsion introduced above a layered more viscous fluid.

The experiments were made at room temperature in rectangular plastic tanks 17 cm in depth and 12×6 cm in area. The lower layer consisted of standard grade corn syrup that was further concentrated by heating and evaporation for several hours, then allowed to cool. By varying the length and temperature of heating, we were able to produce a range of concentrations with dynamical viscosities from 300 to 7000 Pa s and densities from 1200 to 1430 kg m^{-3}. The upper layer consisted of the same syrup diluted with water to reduce its density and viscosity. Typical upper layer viscosities were in the range of 1–10 Pa s, and the density reduction of the upper layer relative to the lower layer was typically 10 per cent. Various dyes were mixed into the upper layer for visualization purposes, including fluorescein dye and blue vegetable dye. The presence of these dyes had no discernible effects on the density or viscosity of either solution.

Gallium liquid has a density of approximately 6000 kg m^{-3} and a viscosity of approximately 2×10^{-3} Pa s near its 29°C melting point. Gallium is a convenient liquid metal for experimentation at room temperatures, however, because its kinetics strongly inhibit freezing while in contact with other liquids such as corn syrups. Gallium reacts with air and with dissolved oxygen to form various gallium oxides, although these oxidation reactions can be largely suppressed for the duration of an experiment by including a small amount of hydrochloric acid in the syrup solution. Liquid gallium has a large interfacial tension in corn syrup, $\sigma\simeq700$ mJ m^{-2}.

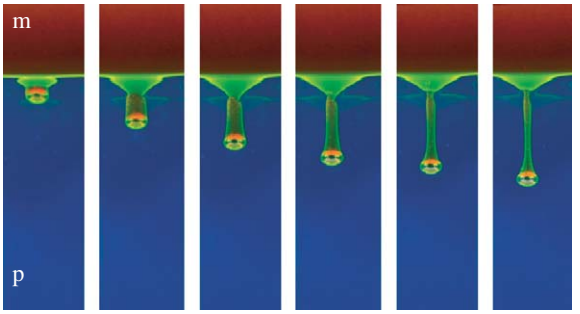

Figure 1. Time sequence showing the motion of a single drop of liquid gallium falling through a two-layer stratified sucrose solution, forming a trailing conduit. Upper low-viscosity fluid (m) appears red, lower high-viscosity fluid (p) appears blue. The low-viscosity fluid appears green when passing through the high-viscosity fluid, illuminating the conduit. The upper/lower layer density and viscosity ratios are 0.9 and 0.01, respectively. The Reynolds and Bond numbers of the gallium drop are 0.01 and 0.3, respectively. Drop diameter is 4.3 mm.

Several dimensionless parameters characterize these experiments. One is the Reynolds number $Re = \rho WR/\eta$, where ρ is density; η is dynamical viscosity of the host fluid; and W is the terminal velocity of a gallium drop of radius R in that fluid. Another parameter is the Bond number $B = \Delta\rho g R^2/\sigma$, where g is gravity and $\Delta\rho$ is the difference between gallium and host fluid densities. Two additional dimensionless parameters that characterize the background stratification are the density ratio ρ_m/ρ_p and the viscosity ratio η_m/η_p. Throughout this paper, the subscripts 'm', 'p' and 'c' denote densities and viscosities of the upper layer (representing the magma), the lower layer (representing the crystalline or 'primitive' mantle) and the metal (core-forming material), respectively. Typical values of the above parameters in our experiments are $Re \sim 10^{-4}$, $\rho_m/\rho_p \simeq 0.9$, $\eta_m/\eta_p \simeq 0.01$ and $B \simeq 0.2-20$. Interfacial tension dominates in the experiments with small values of B, whereas buoyancy effects dominate for large values of B. We use the terms 'drops' and 'diapirs' to describe isolated parcels of liquid gallium falling through the syrup at small and large Bond numbers, respectively.

3. Single-drop experiments

The low-Reynolds-number motion of a liquid drop through a stratified fluid interface is of fundamental importance in a variety of geological and geophysical contexts, as well as industrial situations (Chi & Leal 1989). Experiments on liquid and solid drops falling in a stably stratified fluid have been made for geophysical applications by Manga & Stone (1995) and Srdic-Mitrovic *et al.* (1999) using two-layered and continuously stratified fluid, respectively. The basic phenomena are illustrated by the sequence of images in figure 1. A single drop of liquid gallium is injected from a syringe into the upper (red) layer of the stratified two-layer host fluid. The gallium drop deforms the interface as it approaches the denser and more viscous lower (blue) layer. The drop is surrounded by a film of the upper layer fluid as it falls below the static level of the interface, and a trailing conduit (sometimes called a caudal) forms behind the drop, consisting of fluid entrained from the upper layer. As the drop falls a few of its own diameters into the lower layer, the film of upper layer fluid surrounding

the drop is squeezed back towards the drop's trailing edge and incorporated into the trailing (green) conduit. Because the conduit fluid is soluble in the lower layer, surface tension instabilities do not break the conduit or separate it from the drop. Instead, the conduit remains connected to both the drop and the upper layer as the drop falls a distance corresponding to many of its own diameters. For example, we observed in some experiments that the conduit remained continuously connected for more than 40 drop diameters.

The width of the conduit depends on the drop size and the viscosity and density of the two host fluids. In dynamical terms, the relevant dimensionless parameter is the ratio of the terminal (downward) speed of the drop W to the characteristic (upward) velocity of the buoyant fluid in the conduit w. If w/W is small, then a cylindrical conduit with the same diameter follows the drop. In this situation, the conduit is filled with upper layer fluid that is essentially in hydrostatic equilibrium, as in a stagnant well. Alternatively, if the properties of the lower layer permit the wall of the conduit to constrict by viscous relaxation, then the ratio w/W will not be small. In this situation, the conduit will progressively constrict as the drop falls, as shown in figure 1.

The presence of the conduit causes the terminal velocity of the drop to deviate from the predicted Stokes velocity of the same drop in an infinite homogeneous viscous fluid. For the drop shown in figure 1, the drag on its leading half is well approximated by the Stokes drag, $D^+ = 2\pi\eta_\mathrm{p} R W$, but the drag on its trailing half is different by virtue of the conduit. The effect of the conduit drag on the shape of the drop is not evident in figure 1, since the Bond number in this case is small and interfacial tension tends to keep the drop nearly spherical. In other cases, where both w/W and $\eta_\mathrm{m}/\eta_\mathrm{p}$ are small, the conduit fluid is essentially static and only its pressure deficit contributes to the drag, so that the drag on the trailing half of the drop is $D^- = \pi(\rho_\mathrm{p} - \rho_\mathrm{m}) g R^2 z$, where z is the distance that the drop has fallen below the interface. At low Reynolds number, the sum of these drag forces balances the net weight of the drop F according to

$$D^+ + D^- = F, \tag{3.1}$$

where $F = 2\pi g R^3(\rho_\mathrm{c} - \rho_\mathrm{p})/3$ is the net weight of a semi-spherical half-diapir in the lower fluid. Substituting the expression for F and the two drag factors, (3.1) can be rewritten as an equation for the velocity of the drop as a function of its depth below the interface, or, alternatively, its depth as a function of time t

$$W(z) \equiv \frac{\mathrm{d}z}{\mathrm{d}t} = \frac{(\rho_\mathrm{c} - \rho_\mathrm{p}) g R^2}{3\eta_\mathrm{p}} - \frac{(\rho_\mathrm{p} - \rho_\mathrm{m}) g R}{2\eta_\mathrm{p}} z. \tag{3.2}$$

Provided the conduit remains intact, the second term in (3.2) produces a steady deceleration of the drop with increasing depth below the interface.

Pre-existing low viscosity conduits produced by an initial drop can increase the terminal velocity of subsequent drops and diapirs above that given by (3.2). Figure 2 shows the motion of a drop along a pre-existing conduit. In this case, the conduit reduces the drag on the leading half of the drop, providing a lower resistance descent path. If the Bond number is small (and assuming the fluid through which it descends is not turbulent) the drop remains nearly spherical, as it does in figure 2. However, if the Bond number is large, the diapir deforms into a more streamlined solitary wave shape and descends more rapidly within the conduit (Olson & Singer 1985; Manga & Stone 1995). The influence of

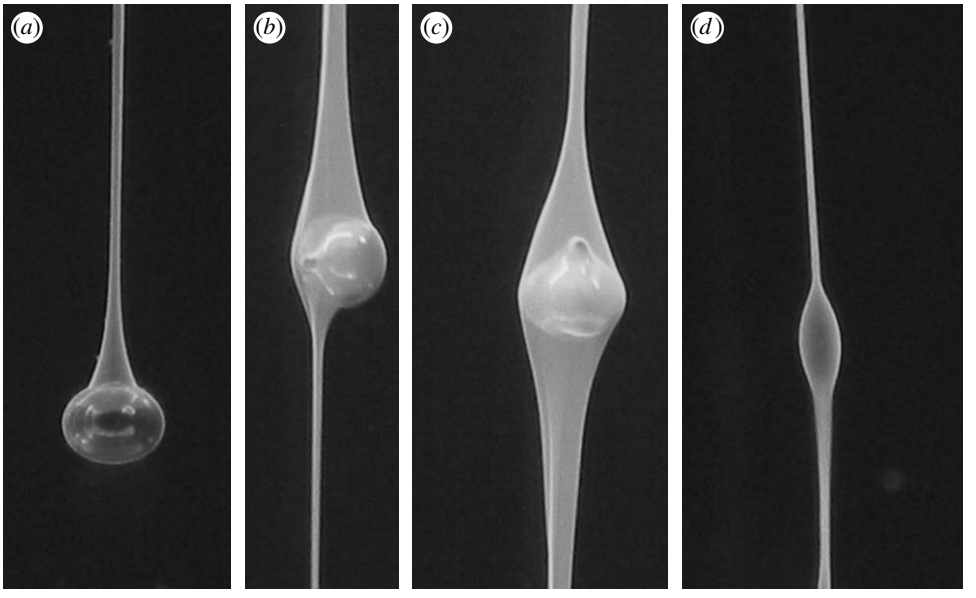

Figure 2. (*a–d*) Sequence showing the plume evolution formed by successive drops of gallium falling through the lower layer of a two-layer stratified sucrose solution. (*a*) Initial plume with gallium head and sucrose tail. (*b*) Second drop falling along the initial conduit. (*c*) Subsequent drop falling along pre-existing conduit. (*d*) Rising streamlined soliton. The upper/lower layer density and viscosity ratios are 0.9 and 0.01, respectively. The Reynolds and bond numbers of the gallium drops are 0.01 and 0.3, respectively. Drop diameters are 4.4 mm.

pre-existing conduits on the terminal velocity is seen in figure 3, which shows the increase in velocity for a succession for equal volume drops descending along the same path. Repeated drops enlarge the low-resistance conduit, and the velocity of successive drops first approaches and then exceeds the Stokes velocity of an inviscid sphere.

4. Instability of a metal pond

If the core-forming metal derived from a large planetesimal object remains coherent following impact, it will quickly sink to the base of the magma ocean and pond at the top of the highly viscous primitive mantle. If the metal pond formed this way is shallow compared with its lateral dimension, subsequent gravitationally induced motion will approximate the classical Rayleigh–Taylor instability of a thin dense layer above a less dense but more viscous fluid (Chandrasekhar 1961; Whitehead & Luther 1975). In the three-layer system envisoned for the early Earth, the Rayleigh–Taylor instability is controlled by the material properties of the most viscous region (i.e. the viscosity and density of the primitive mantle) and the density of the metal (Solomatov 2000). The characteristic growth time of a Rayleigh–Taylor instability in this situation depends inversely on the wavelength of the disturbance λ and is approximately

$$t_{\mathrm{RT}} \simeq \frac{2\pi\eta_{\mathrm{p}}}{(\rho_{\mathrm{c}} - \rho_{\mathrm{p}})g\lambda}. \tag{4.1}$$

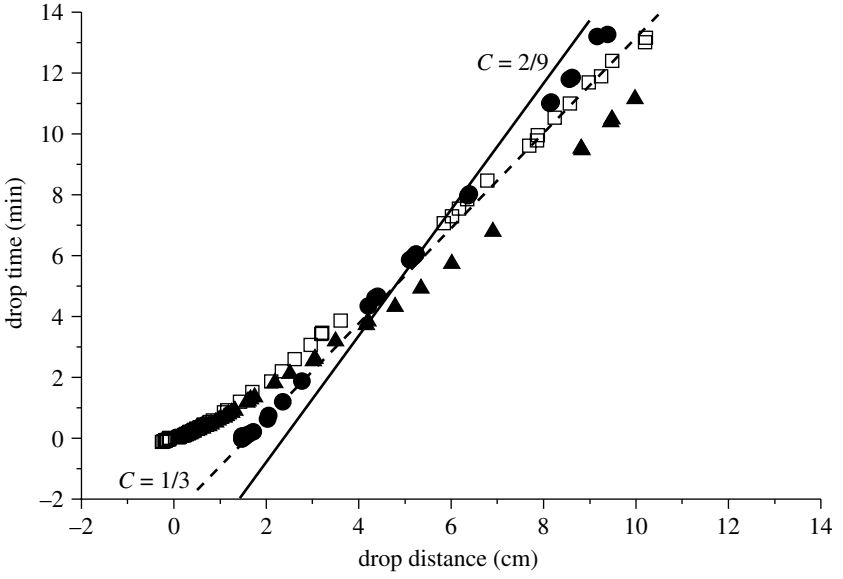

Figure 3. Distance versus time plot showing the motion of liquid gallium drops in the lower layer of a two-layer stratified sucrose solution. Distance and time are measured from the fluid–fluid interface. Circles, gallium drop in a homogeneous fluid; squares, initial drop in a stratified fluid; triangles, second drop in the same stratified fluid. The upper/lower density and viscosity ratios are 0.9 and 0.01, respectively. The Reynolds and Bond numbers of the gallium drop are 0.01 and 0.3, respectively. Dashed and solid lines show theoretical Stokes velocity for an inviscid ($C=1/3$) and a rigid ($C=2/9$) sphere, respectively.

Formulae equivalent to (4.1) have been derived by Canright & Morris (1993) for Cartesian geometry and by Ribe & de Valpine (1994) for the Rayleigh–Taylor instability of a thin, dense, low-viscosity layer in a more viscous, less dense spherical shell.

Metal ponds are expected to form at the base of a magma ocean following large impacts if the settling time for metal in the magma ocean is short compared with t_{RT}, as it is likely to be (Reese & Solomatov 2006). The situation may be different for small objects, or large objects that disaggregate on impact. Depending on the size of the metal drops, the time of settling and compaction at the base of the magma ocean may not be short when compared with t_{RT}, in which case the instability involves a metal–silicate emulsion. This situation will be considered in §5.

Figure 4 shows a sequence of images from a Rayleigh–Taylor instability developing in a layer of liquid gallium between thicker layers of dilute and concentrated syrup. The gallium layer thickness is initially $h=0.5$ cm and the upper and lower layer viscosities are $\eta_{\mathrm{m}}=10$ and $\eta_{\mathrm{p}}=6000$ Pa s, respectively. The wavelength of the instability predicted for (4.1) is comparable to the tank dimension, and we find the least stable mode is wavenumber one or two. The close-ups in figure 5 show the segmentation of the gallium layer by the finite amplitude Rayleigh–Taylor instability. Segmentation occurs at the location of upwelling in the lower viscous fluid. In our experiments, these upwellings typically were found at a distance equal to one-quarter of the tank width from one of the boundaries, and split the gallium layer into two parts with volumes in the approximate ratio of 3 : 1.

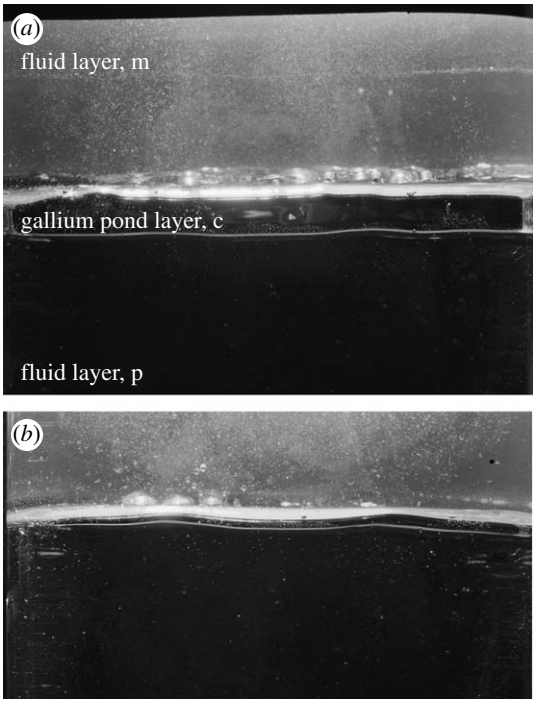

Figure 4. (*a*) Onset of Rayleigh–Taylor instability of a liquid gallium layer between two less dense but more viscous sucrose solution layers. The upper/lower density and viscosity ratios are 0.9 and 0.01, respectively, and the gallium layer thickness is initially 0.7 cm (t=0 hours). (*b*) Later in time (t=4 hours).

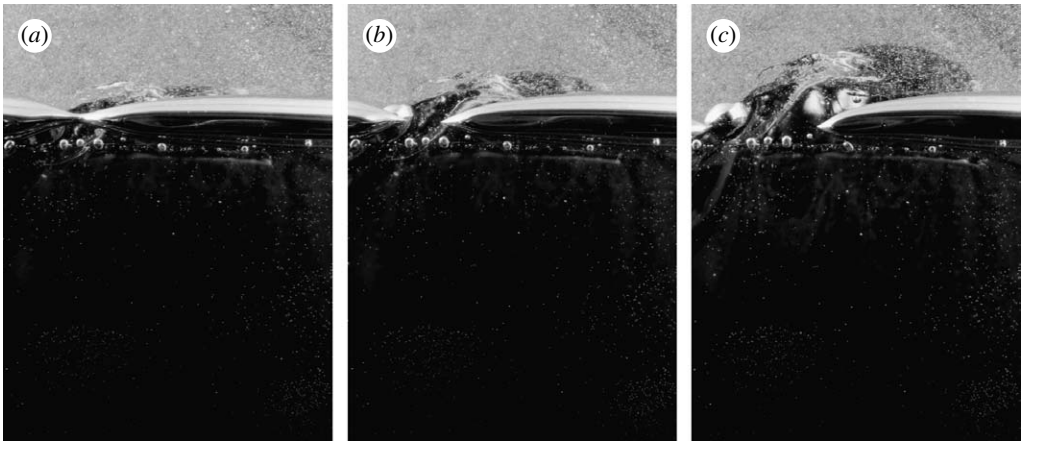

Figure 5. (*a–c*) Time sequence showing gallium layer segmentation during Rayleigh–Taylor instability of the three-layer fluid system in figure 4.

Figure 6 shows how the Rayleigh–Taylor instability evolves in time. Here, the Bond number is large, and the dominance of gravity over surface tension effects at the flattened trailing edges of the metal instabilities is clearly evident. In this paper, we use the term 'half-diapir' to describe the shape of the leading metal in

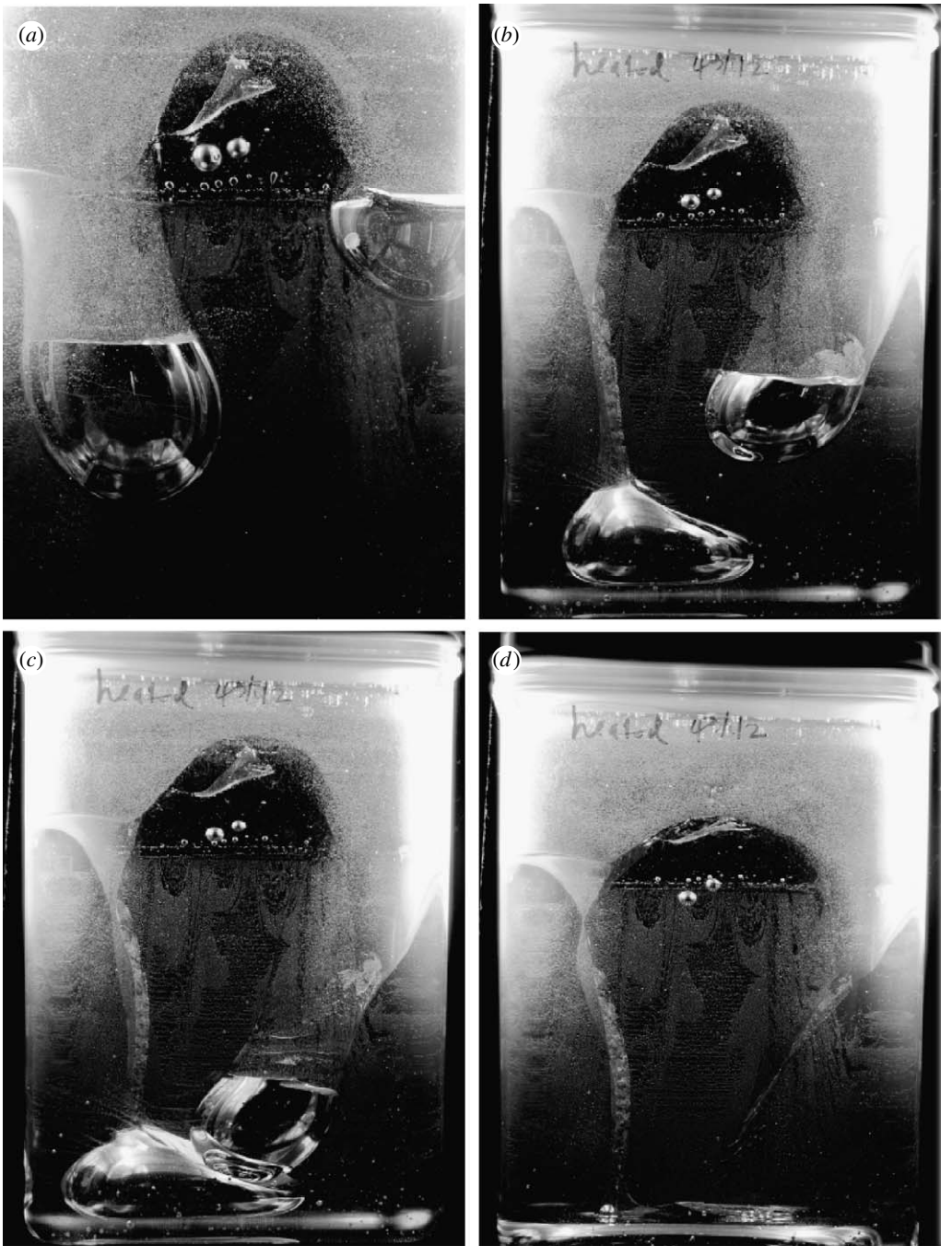

Figure 6. (*a–d*) Time sequence showing the development of half-diapirs and trailing conduits following Rayleigh–Taylor instability of a liquid gallium layer between two less dense but more viscous sucrose solution layers. Gallium diapir diameter on (*a*,*c*) is 4.5 cm. Total descent time from (*a*) to (*d*) is 10 min.

large Bond number metal–silicate plumes with trailing conduits. In this particular experiment, $Re \simeq 10^{-4}$, $B \simeq 20$ and $\eta_{\mathrm{m}}/\eta_{\mathrm{p}} \ll 1$, the set of conditions in which the Rayleigh–Taylor instability produces half-diapirs with large trailing

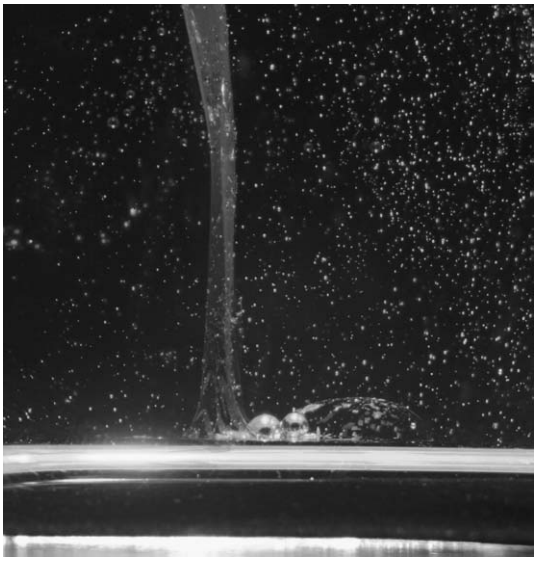

Figure 7. Structure of a positively buoyant thermochemical plume evolved from the trailing conduit of a negatively buoyant gallium plume.

conduits. The flat trailing edges of the metal half-diapirs indicate that the conduits are filled with essentially static upper layer fluid. As the half-diapirs approach the base of the tank and collapse (this is the experimental equivalent to merging with the growing core) the trailing conduits constrict and the net transport direction in these structures reverses from downward to upward. In spite of this flow reversal, the conduits remain partially open long after the metal diapir has collapsed, providing a path for upper layer fluid entrained by the instability to drain back up to the upper layer. In one experiment, we applied heat to the base of the tank after the collapse of the metal half-diapir, and observed that the residual conduit was evolved into a positively buoyant thermal plume, as shown in figure 7.

5. Instability of a dense emulsion

The excess abundance of some siderophile elements in the mantle is evidence that some degree of metal–silicate equilibration at elevated temperature and pressure occurred prior to final core segregation. Since chemical equilibration between liquids is diffusion controlled, it is often supposed that much of the iron that formed the core was dispersed as fine droplets in the magma ocean, and underwent partial phase separation whereby the metals became concentrated at the magma ocean base (Rubie *et al.* 2003; Wood *et al.* 2006). Processes involved in gravitationally driven phase separation in immiscible fluids with large viscosity contrasts have been investigated by Sato & Sumita (2007). Here, we are concerned with the gravitational instability of a dense layer in which the phase separation is incomplete. A related phenomenon is the Rayleigh–Taylor instability of fluids containing particles or bubbles, which has been examined in the context of magma mixing (Thomas *et al.* 1993; Michioka & Sumita 2005)

and sedimenting suspensions (Voltz *et al.* 2000). Depending on the properties of the mixture, either sediment plumes or sediment fingers are observed to form. If the size distribution of the heavy drops is not uniform, as would be the case if the drops formed from the disaggregation of a large parent body, then the largest of the heavy drops will dictate the timing and the type of instability that results.

To demonstrate this effect, we synthesized dense emulsions by shaking mixtures of gallium and diluted syrup solution. The gallium became the dispersed phase, forming drops, while the syrup solution became the continuous phase. The size spectrum of the gallium drops produced this way is non-uniform and depends on the duration of the shaking, i.e. the total kinetic energy input to the emulsion. In particular, there is always one or more larger residual gallium masses present. We then repeated the Rayleigh–Taylor experiments described above, using this emulsion as the upper layer fluid.

Figure 8 shows the instability of a layer of gallium emulsion above a less dense but more viscous syrup layer. A Rayleigh–Taylor instability with the same wavenumber is observed in this case as in the homogeneous gallium layer experiment, and it occurs approximately on the same time scale. The main reason for this correspondence is that the largest gallium volumes coalesce into half-diapirs, which form the leading edge of the resulting plumes. The primary difference in this case is that the trailing conduit contains enough gallium drops to give it overall negative buoyancy in the lower layer. After the leading half-diapir reaches the base of the tank, the smaller gallium drops in the trailing conduit gradually sediment out, reducing the bulk density of the conduit. In all of our emulsion experiments, we find that small emulsion drops in the leading edge coalesce during descent into a cohesive fluid gallium front (figure 8) that behaves similar to the large diapir experiments in figure 6. If no additional gallium is added to the system, the flow in the conduit eventually reverses and it drains back into the upper layer. However, if another dose of emulsion is added to the system at this stage, it descends down one of the established conduits. With repeated doses of emulsion, the conduits can be kept open for long periods of time. In some cases, the conduits develop a grossly heterogeneous structure, in which gallium-rich emulsion descends in one part of the conduit while buoyant, gallium-depleted emulsion ascends in another part, while, in other cases, no such heterogeneity was observed. In principle, it is possible for these structures to reach a statistical steady state, in which the downward transport of metal drops equals the input metal flux and the net transport of lower density diluted syrup solution is zero. Metal–silicate plumes in the early Earth equivalent to these structures would have very high temperatures, owing to the concentrated volumetric heating caused by the viscous dissipation of kinetic energy of the falling metal drops, an effect that is not significant on the scale of these experiments.

6. Metal–silicate mantle plumes

Our experiments suggest the following conceptual model for metal–silicate mantle plumes during core formation. Plume formation is initiated by long wavelength Rayleigh–Taylor instability of a liquid-rich iron pond or a partly

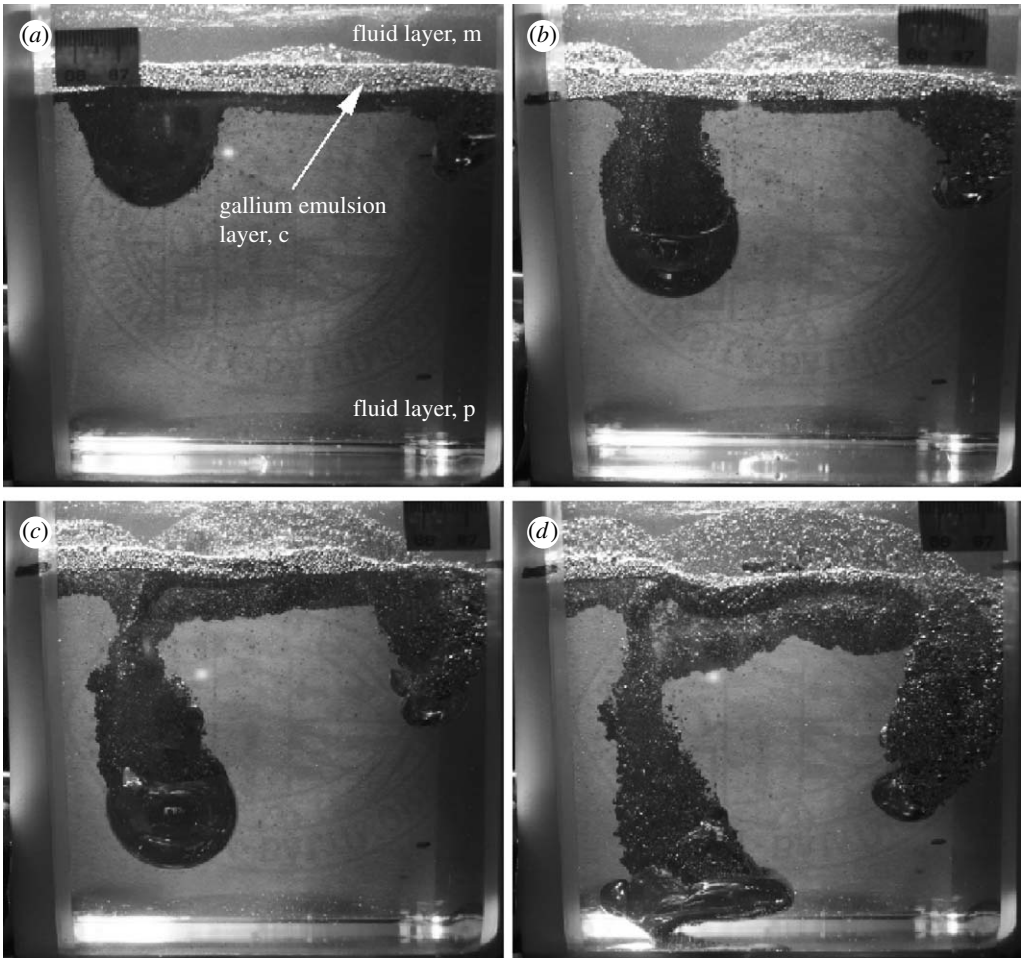

Figure 8. (*a*,*b*) Time sequence showing the development of Rayleigh–Taylor instability of an initial gallium emulsion layer between two less dense but more viscous sucrose solution layers. (*c*,*d*) The growth of a gallium emulsion plume; the upper/lower density and viscosity ratios are 0.9 and 0.01, respectively, and the initial emulsion layer thickness is 1.0 cm. Scale is visible near the upper fluid layer. Total experiment time from (*a*) to (*d*) is 52 min.

segregated iron emulsion layer at the base of the magma ocean. Depending on the lateral extent of the pond layer, each Rayleigh–Taylor instability produces one or more metal diapirs that sink into the highly viscous primitive lower mantle. Trailing conduits filled with magma ocean material are then entrained into the primitive mantle behind each diapir. The material in the conduit is assumed to be a mixture of silicate magma and drops of core-forming metals, and initially these conduits have the same radius as their leading diapir. Provided the magma ocean viscosity η_{m} is very small compared with the primitive mantle viscosity η_{p}, the fluid in the trailing conduit remains in nearly hydrostatic equilibrium, its contribution to viscous drag on the diapir is negligible, and the trailing edge of the diapir is flat. While the metal half-diapirs descend into the primitive mantle, their rates of sinking are governed by (3.2). The evolution of the trailing conduits

depends on the properties of the primitive mantle and the conduit material. If the material in the conduit is less dense and much less viscous than the primitive mantle, the conduit radius a will constrict on a time scale given by

$$t_{\text{conduit}} = \frac{\eta_{\text{p}}}{(\rho_{\text{p}} - \rho_{\text{m}})ga}. \tag{6.1}$$

This is to be compared with the characteristic descent time of the metal diapir through the primitive mantle. Denoting the radial depth of the primitive mantle by L, the diapir descent time is approximately $t_{\text{descent}} = L/W$, where

$$W = \frac{(\rho_{\text{c}} - \rho_{\text{p}})gR^2}{3\eta_{\text{p}}} \tag{6.2}$$

is the Stokes velocity of a half-diapir in the primitive mantle. If $t_{\text{descent}} \ll t_{\text{conduit}}$, that is, if

$$\frac{\rho_{\text{p}} - \rho_{\text{m}}}{\rho_{\text{c}} - \rho_{\text{p}}} \ll \frac{a}{L}, \tag{6.3}$$

then the conduit radius will conform to the half-diapir radius R until the half-diapir reaches the core–mantle boundary. On the other hand, if $t_{\text{descent}} \gg t_{\text{conduit}}$ the conduit will constrict before the diapir reaches the core. A third possibility can occur if the conduit is denser than the primitive mantle owing to a high concentration of core-forming material in the conduit. In this case, the metal drains through the conduit into the diapir and the mass of the diapir increases during its descent.

Previous studies of core formation by Rayleigh–Taylor instability of a uniform, global metal layer above the high viscosity of the primitive mantle (Elsasser 1963; Stevenson 1990) concluded that the most unstable mode corresponds to either a single diapir (mode $m=1$ instability) or, alternatively, a small number of diapirs. Diapirs formed this way would be too large to equilibrate with the primitive mantle during their descent, because only a small fraction of the metal in a sinking diapir circulates through the thin contact region where the chemical and thermal exchanges with the mantle occurs. The characteristic distance a diapir must travel to equilibrate with its surroundings by the mixing action of its own internal circulation is given by $R^2 W/\kappa$, where κ is the relevant diffusivity (heat or mass) and W is the Stokes velocity (6.2). The R^4 dependence implied by this expression means that only rather small diapirs or drops will equilibrate in descent through the primitive mantle. Another implication is that diapirs small enough to mix by their own internal Stokes flow would solidify in the relatively low temperature primitive mantle long before they reached chemical equilibration, because, except for the light elements helium and hydrogen, the diffusivity of heat is of the orders of magnitude larger than mass diffusion.

Chemical equilibrium during core formation requires small metal drop sizes, and, in order for the metal to remain liquid, the temperature must be high. Here, we demonstrate that it is possible to maintain such an environment in an equilibrium metal–silicate mantle plume conduit. Figure 9 is a sketch of an idealized fully developed metal–silicate plume conduit with an assumed circular

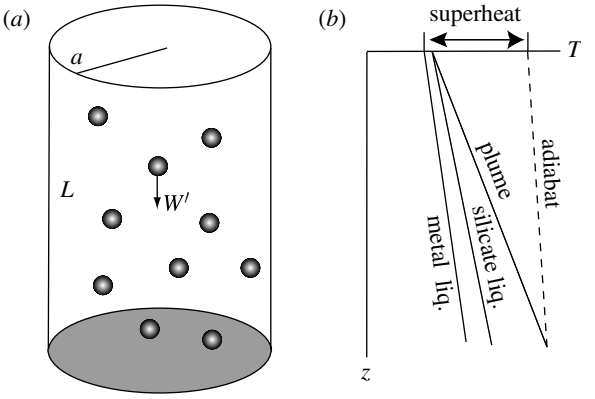

Figure 9. (*a*) Sketch of a steady-state metal–silicate mantle plume conduit used in the analysis, showing liquid metal drops sinking through a silicate magma matrix. (*b*) Schematic distribution of temperature along the plume, including metal and silicate melting lines, metal adiabat, plume temperature profile and core superheat.

cross section, containing a mixture of liquid core-forming metal and silicate melt. We use χ to represent the mass fraction of metals in the plume, which we assume are dispersed in the silicate melt in the form of individual drops. In reality there will always be a distribution of drop sizes, but in this analysis we consider for purposes of simplicity a uniform drop size with a spherical radius R'. We assume that the metal is drawn from the magma ocean into the conduit and descends through the conduit as a cloud of individual Stokes drops all the way to the core.

The conservation of mass for the core-forming material in the conduit can be written

$$\rho_{\rm c}(W' + w)\chi A = F_{\rm c}, \tag{6.4}$$

where $A = \pi a^2$ is the plume cross-sectional area; $F_{\rm c}$ is the mass flux of core-forming metal into the plume;

$$W' = \frac{(\rho_{\rm c} - \rho_{\rm m})gR'^2}{3\eta_{\rm m}} \tag{6.5}$$

is the Stokes velocity in the conduit for the metal drops; and w is the average velocity of the silicate magma in the plume.

We are particularly interested in the limiting case of low metal concentration ($\chi \ll 1$) and negligible magma transport, i.e. $w \simeq 0$ in (6.4). This later condition is met when the conduit mixture is neutrally buoyant with respect to the primitive mantle. The addition of metal will tend to evolve an otherwise positively buoyant silicate melt plume towards a state of neutral buoyancy, for dynamical reasons. If the conduit material is initially less dense on average than the surrounding primitive mantle, it will constrict, thereby increasing its metal concentration and its density. Neutral buoyancy of the plume mixture relative to the primitive mantle corresponds to a metal concentration of

$$\chi = \frac{\rho_{\rm p} - \rho_{\rm m}}{\rho_{\rm c} - \rho_{\rm m}}. \tag{6.6}$$

According to (6.4), (6.5) and (6.6), the equilibrium cross-sectional area of a neutrally buoyant plume conduit is

$$A = \frac{3\eta_{\rm m} F_{\rm c}}{\rho_{\rm c}(\rho_{\rm p} - \rho_{\rm m}) g R'^2}. \tag{6.7}$$

The relative motion of the metal drops with respect to the magma provides the major source of heating in the plume, through viscous dissipation. The amount of dissipative heating in the plume can be estimated from the change in gravitational potential energy due to the Stokes velocity of the metal drops. For a single drop falling at a speed given by (6.5), the rate of gravitational energy release is

$$Q = \frac{4\pi(\rho_{\rm c} - \rho_{\rm m})^2 g^2 R'^5}{\eta_{\rm m}}. \tag{6.8}$$

Assuming that all the energy released this way goes into viscous heat (this is a reasonably good assumption for Stokes flow around isolated drops), the rate of volumetric heat production in the plume from a uniform distribution of such drops is given by

$$\epsilon = \frac{3\chi Q}{4\pi R'^3} = \frac{3(\rho_{\rm c} - \rho_{\rm m})^2 g^2 \chi R'^2}{\eta_{\rm m}}. \tag{6.9}$$

This result can be used to estimate the superheat acquired by metal drops descending from the magma ocean to the core through the conduit. Ignoring heat conduction, the change in temperature with time for a metal drop falling through the conduit consists of an adiabatic increase (denoted by subscript *ad*) plus the superadiabatic temperature increase due to the viscous heating (denoted by subscript *sa*), and is given by

$$\frac{{\rm d}T}{{\rm d}t} = W' \frac{{\rm d}T}{{\rm d}z}\Big|_{\rm ad} + \frac{{\rm d}T}{{\rm d}t}\Big|_{\rm sa} = \frac{\gamma T W'}{H_T} + \frac{\epsilon}{\rho_{\rm m} C_{\rm p}}, \tag{6.10}$$

where γ is the Gruneisen parameter and $H_T = C_{\rm p}/\alpha g$ is the temperature scale height (here $C_{\rm p}$ and α are specific heat and thermal expansivity of the magma in the plume, respectively). According to (6.5), (6.6) and (6.10) the superadiabatic temperature increase due to viscous heating experienced by a metal drop falling in a conduit a distance L at a speed W' is approximately

$$\Delta T_{\rm sa} = \frac{\epsilon L}{\rho_{\rm m} C_{\rm p} W'} = \frac{9(\rho_{\rm p} - \rho_{\rm m}) g L}{\rho_{\rm m} C_{\rm p}}. \tag{6.11}$$

Although the viscous heat production (6.9) depends on the magma viscosity, which is poorly constrained, the intrinsic superadiabatic temperature increase experienced by the falling drops (6.11) is independent of this viscosity. It also has no explicit dependence on the metal properties, a consequence of assuming neutral conduit buoyancy.

The amount of core superheat that would result from this style of metal segregation is probably quite large. Using the parameter values in table 1, (6.11) gives $\Delta T_{\rm sa} = 3200$ K. This is far in excess of the increase in metal and silicate

Table 1. Metal–silicate mantle plume model properties.

inputs	notation	units	assumed value
metal mass flux	F_c	$kg\,s^{-1}$	6×10^{8}
magma density	ρ_m	$kg\,m^{-3}$	3.9×10^{3}
primitive mantle density	ρ_p	$kg\,m^{-3}$	4.0×10^{3}
core-forming metal density	ρ_c	$kg\,m^{-3}$	9×10^{3}
magma viscosity	η_m	Pa s	1×10^{7}
primitive mantle viscosity	η_p	Pa s	1×10^{23}
gravity	g	$m\,s^{-2}$	9
metal drop radius	R'	m	0.1
mass diffusivity	κ	$m^2\,s^{-1}$	1×10^{-10}
primitive mantle depth	L	m	2×10^{6}
results			calculated value
plume, metal diapir radii	a, R	km	265
metal concentration (conduit)	χ	n.d.	0.02
viscous heating (conduit)	ϵ	$W\,m^{-3}$	0.125
metal superheat (conduit)	ΔT_{sa}	K	3200
Rayleigh–Taylor instability time	t_{RT}	Myr	1
diapir descent time	t_{diapir}	Myr	6
drop descent time (conduit)	t_{drop}	Kyr	4
conduit constriction time	$t_{conduit}$	Myr	17.6
mass diffusion radius	R'_{crit}	m	0.6

liquidus temperatures across the pressure interval of the primitive mantle, which ensures that metal–silicate plume conduits would remain entirely molten. Note that we have assumed a small density difference between the primitive mantle and the conduit magma; larger differences imply even more dissipative heating in the plume. The actual superheat of the core formed this way would be smaller than ΔT_{sa}, however, for several reasons. First, we have ignored the effects of heat diffusion from the plume in the above analysis. Second, the metal diapirs that produce these conduits may not experience as much superheating in the course of their descent through the primitive mantle. And finally, if the proto-Earth already had a small core, that metal was probably at a lower temperature than the incoming metal.

In table 1 a nominal metal drop size of 0.1 m is assumed. We can estimate the threshold radius for a drop to chemically re-equilibrate with the magma in the conduit by equating its characteristic mass diffusion time R'^2/κ to its descent time, $t_{drop} = L/W'$. This criterion predicts that a drop will not chemically re-equilibrate with the conduit magma if its radius far exceeds

$$R'_{crit} = \left[\frac{3\kappa\eta_m L}{(\rho_c - \rho_m)g}\right]^{1/4}. \tag{6.12}$$

Using the parameter values in table 1, $R'_{crit} \simeq 0.25$ m, an estimate that is sensitive to the assumed mass diffusivity and the viscosity of the conduit material. On the other hand, drops for which $R' \ll R'_{crit}$ could locally equilibrate with the surrounding magma as a function of depth.

Other properties of metal–silicate plumes can be estimated from this model using the parameter values in table 1. According to (6.6), the concentration of metals in a neutrally buoyant conduit is $\chi \simeq 0.02$. The steady-state cross-sectional area of a neutrally buoyant metal–silicate plume depends on the mass flux of metal into the conduit, according to (6.7). Core formation lasting 20 Myr corresponds to a time average metal mass flux of nearly $3\times10^{9}\ \mathrm{kg\,s^{-1}}$, assuming the initial core mass was negligible compared with its final mass. The value $F_{\mathrm{c}}=6\times10^{8}\ \mathrm{kg\,s^{-1}}$ in table 1 corresponds to five equal-sized plumes active over the 20 Myr period. According to (6.7), the radius of each plume would be approximately 265 km. The time required to create such a plume is given by the growth time of the initial instability plus the descent time of a half-diapir with this same radius. Using (6.2), the parameter values in table 1 give $t_{\mathrm{diapir}} \simeq 6$ Myr for the descent time and, according to (4.1), the growth rate of the initial instability would be of order 1 Myr or less. These are to be compared with the constriction time of the trailing conduit. If the conduit consisted only of silicate magma with the property values in table 1, then $t_{\mathrm{conduit}} \simeq 17.6$ Myr. This might be an underestimate, since it is likely that the conduit would also contain some core-forming metal, which would reduce its density deficit relative to the primitive mantle and increase the constriction time. In any case, the metal–silicate plume would be fully developed within the requisite 20 Myr period, provided the primitive mantle viscosity was not too much larger than the 10^{23} Pa s assumed in this model.

7. Discussion

Our experiments indicate that large iron diapirs sinking through a magma ocean into the viscous primitive lower mantle form trailing conduits filled with the upper mantle silicate melts and metal drops. The large iron diapirs could originate from major impact events involving differentiated planetesimals, or through Rayleigh–Taylor instabilities of metal ponds or emulsions concentrated at the base of the magma ocean. The molten conduits provide a low-resistance path for additional metal transport through the high-viscosity primitive mantle. Metal-rich silicate plumes are highly dissipative due to viscous heating provided by the falling metal drops, which facilitates high-pressure metal–silicate equilibrium in the conduit and strongly superheats the metal drops before they enter the core.

We can speculate how metal–silicate plumes might evolve following the main phase of core formation. As the flux of core-forming metal through the plume decreases, the net buoyancy of the plume material would become positive in the primitive mantle. The overall flow in the plume would then be upward and the silicate melt in the conduit would drain back towards the Earth's surface. When the flow direction in the metal-depleted plumes reversed, they would begin to extract some of the superheat from the core. This process could serve to initiate the geodynamo, by establishing a regime of thermal convection in the core shortly after the main phase of core formation. The change from neutrally buoyant metal–silicate plumes relatively rich in core-forming metals to positively buoyant plumes relatively depleted in core-forming metals is likely to be a gradual transition, which might be expected to recycle significant amounts of

metals back towards the Earth's surface. Reversal in the direction of core-forming plumes offers an explanation for why there were major pulses of volcanic activity and heterogeneous crust formation in the early history of some terrestrial planets, such as has been proposed for the crustal dichotomy on Mars (Ke & Solomatov 2006). It also suggests that plumes may have been the initial phase of whole mantle convection in the Earth.

This research was supported by grant EAR-0604974 from the Geophysics Program of the National Science Foundation. D.W. was supported by the Carnegie Institution of Washington and by the NASA Planetary Geology and Geophysics Program under grant NNX07AP50G.

References

Canright, D. & Morris, S. 1993 Buoyant instability of a viscous film over a passive fluid. *J. Fluid Mech.* **255**, 349–372. (doi:10.1017/S0022112093002514)

Chabot, N. L., Draper, D. S. & Agee, C. B. 2005 Conditions of core formation in the Earth: constraints from nickel and cobalt partitioning. *Geochim. Cosmochim. Acta* **69**, 2141–2151. (doi:10.1016/j.gca.2004.10.019)

Chandrasekhar, S. 1961 *Hydrodynamic and hydromagnetic stability*, p. 652. New York, NY: Dover.

Chi, B. K. & Leal, L. G. 1989 A theoretical study of the motion of a viscous drop toward a fluid interface at low Reynolds number. *J. Fluid Mech.* **201**, 123–146. (doi:10.1017/S0022112089000868)

Elsasser, W. M. 1963 Early history of the Earth, dedicated to F.G. Houtermans on his sixtieth birthday. In *Earth science and meteroitics* (eds J. Geiss & E. Goldberg), pp. 1–30. New York, NY: Elsevier.

Honda, R., Mizutani, H. & Yamamoto, T. 1993 Numerical simulations of Earth's core formation. *J. Geophys. Res.* **98**, 2075–2089. (doi:10.1029/92JB02699)

Ida, S. Y., Nakagawa, Y. & Nakazawa, K. 1987 The Earth's core formation due to Rayleigh–Taylor instability. *Icarus* **69**, 239–248. (doi:10.1016/0019-1035(87)90103-5)

Ke, Y. & Solomatov, V. S. 2006 Early transient superplumes and the origin of the Martian crustal dichotomy. *J. Geophys. Res.* **111**, E10001. (doi:10.1029/2005JE002631)

Klein, T., Munker, C., Mezger, K. & Palme, H. 2002 Rapid accretion and early core formation on astroids and the terrestrial planets from Hf–W chronometry. *Nature* **418**, 952–955. (doi:10.1038/nature00982)

Labrosse, S., Poirier, J. P. & LeMouel, J. L. 2001 The age of the inner core. *Earth Planet. Sci. Lett.* **190**, 111–123. (doi:10.1016/S0012-821X(01)00387-9)

Manga, M. & Stone, H. A. 1995 Low Reynolds number motion of bubbles, drops and rigid spheres through fluid–fluid interfaces. *J. Fluid Mech.* **287**, 279–298. (doi:10.1017/S0022112095000954)

Michioka, H. & Sumita, I. 2005 Rayleigh–Taylor instability of a packed viscous fluid: implications for a solidifying magma. *Geophys. Res. Lett.* **32**, L03309. (doi:10.1029/2004GL021827)

Nimmo, F. 2007 Energetics of the core In *Treatise on geophysics*, vol. 8 (ed. P. Olson). Core dynamics, pp. 31–66. New York, NY: Elsevier B.V.

Olson, P. & Singer, H. 1985 Creeping plumes. *J. Fluid Mech.* **158**, 511–531. (doi:10.1017/S0022112085002749)

Reese, C. C. & Solomatov, V. S. 2006 Fluid dynamics of local martian magma oceans. *Icarus* **184**, 102–130. (doi:10.1016/j.icarus.2006.04.008)

Ribe, N. M. & de Valpine, D. P. 1994 The global hotspot distribution and instability of D''. *Geophys. Res. Lett.* **21**, 1507–1510. (doi:10.1029/94GL01168)

Righter, K. & Drake, M. J. 2000 Metal/silicate equilibrium in the early Earth—new constraints from the volatile moderately siderophile elements Ga, Cu, P and Sn. *Geochim. Cosmochim. Acta* **64**, 3581–3597. (doi:10.1016/S0016-7037(00)00466-X)

Rubie, D. C., Melosh, H. J., Reid, J. E., Liebske, C. & Righter, K. 2003 Mechanisms of metal–silicate equilibration in the terrestrial magma ocean. *Earth Planet. Sci. Lett.* **205**, 239–255. (doi:10.1016/S0012-821X(02)01044-0)

Rubie, D. C., Nimmo, F. & Melosh, H. J. 2007 Formation of Earth's core. In *Treatise on geophysics*, vol. 9 (ed. D. Stevenson). Evolution of the Earth, pp. 51–90. New York, NY: Elsevier B.V.

Sato, M. & Sumita, I. 2007 Experiments on gravitational phase separation of binary immiscible fluids. *J. Fluid Mech.* **591**, 289–319. (doi:10.1017/S0022112007008257)

Solomatov, V. S. 2000 Fluid dynamics of magma oceans. In *Origin of the Earth and Moon* (eds R. Canup & K. Righter), pp. 323–338. Tucson, AZ: University of Arizona Press.

Srdic-Mitrovic, A. N., Mohamed, N. A. & Fernando, H. J. S. 1999 Gravitational settling of particles through density interfaces. *J. Fluid Mech.* **381**, 175–198. (doi:10.1017/S0022112098003590)

Stevenson, D. J. 1990 Fluid dynamics of core formation. In *Origin of the Earth* (eds N. E. Newsom & J. H. Jones), pp. 231–249. New York, NY: Oxford University Press.

Thomas, N., Tait, S. & Koyaguchi, T. 1993 Mixing of stratified liquids by motion of gas bubbles: applications to magma mixing. *Earth Planet. Sci. Lett.* **115**, 161–175. (doi:10.1016/0012-821X(93)90220-4)

Voltz, C., Schroter, M., Iori, G., Betat, A., Lange, A., Engel, A. & Rehber, I. 2000 Finger-like patterns in sedimening water–sand suspensions. *Phys. Rep.* **337**, 117–138. (doi:10.1016/S0370-1573(00)00058-2)

Whitehead, J. A. & Luther, D. S. 1975 Dynamics of laboratory diapir and plume models. *J. Geophys. Res.* **80**, 705–717. (doi:10.1029/JB080i005p00705)

Wood, B. J., Walter, M. J. & Wade, J. 2006 Accretion of the Earth and segregation of its core. *Nature* **441**, 825–833. (doi:10.1038/nature04763)

Yoshino, T., Walter, M. J. & Katsura, T. 2003 Core formation in planetesimals triggered by permeable flow. *Nature* **422**, 154–157. (doi:10.1038/nature01459)